PhotoniX

RESEARCH Open Access

Spectral period doubling and encoding of dissipative optical solitons via gain control

Kangwen Yang[1,2,3†], Yi Zhou[2,3*†], Yuqing Ling[1], Kevin K. Tsia[2,3], Heping Zeng[4*] and Kenneth K. Y. Wong[2,3*]

†Kangwen Yang and Yi Zhou contributed equally to this work.

*Correspondence: zhouyi08@hku.hk; hpzeng@phy.ecnu.edu.cn; kywong@eee.hku.hk

[1] Shanghai Key Laboratory of Modern Optical System, and Engineering Research Center of Optical Instrument and System, Ministry of Education, School of Optical Electrical and Computer Engineering, University of Shanghai for Science and Technology, Shanghai 200093, China
[2] Department of Electrical and Electronic Engineering, The University of Hong Kong, Hong Kong, China
[3] Advanced Biomedical Instrumentation Centre, Hong Kong Science Park, Hong Kong, China
[4] State Key Laboratory of Precision Spectroscopy, East China Normal University, Shanghai 200062, China

Abstract

Period-doubling bifurcation, as an intermediate state between order and chaos, is ubiquitous in all disciplines of nonlinear science. However, previous experimental observations of period doubling in ultrafast fiber lasers are mainly restricted to self-sustained steady state, controllable manipulation and dynamic switching between period doubling and other intriguing dynamical states are still largely unexplored. Here, we propose to expand the vision of dissipative soliton periodic doubling, which we illustrate experimentally by reporting original spontaneous, collisional, and controllable spectral period doubling in a polarization-maintaining ultrafast fiber laser. Specifically, the spontaneous period doubling can be observed in both single- and double-pulses. The mechanism of the switchable state and periodic doubling was revealed by numerical simulation. Moreover, state transformation of individual solitons can be resolved during the collision of triple solitons involving stationary, oscillating, and period doubling. Further, controllable deterministic switching between period doubling and other dynamical states, as well as exemplifying the application of period-doubling-based digital encoding, is achieved under programmable pump modulation. Our results open a new window for unveiling complex Hopf bifurcation in dissipative systems and bring useful insights into nonlinear science and applications.

Keywords: Period doubling, Mode locking, Ultrafast fiber lasers

Introduction

Dissipative solitons in nonlinear mediums arise from the complex balance between nonlinearity and dispersion, as well as gain and loss [1]. As universal in nature, dissipative solitons have been found in various fields of natural science, such as ecosystems, biology, fluid dynamics, and chemistry [2]. In addition to parameter-invariant stationary solitons, many nonlinear systems support pulsating or oscillating solitons, the energy of which is localized in space but oscillates in time, or vice versa. Mode-locked laser, as an absolutely dissipative system, provides an ideal platform to explore versatile soliton dynamics with a virtually infinite number of degrees of freedom. Plentiful nonlinear phenomena have been observed in mode-locked lasers, including pulsation soliton [3–5], soliton molecules [6–9], soliton explosion [10, 11], soliton collision [12, 13], and optical rogue waves [14, 15]. Especially, period-doubling bifurcation, as a particularly soliton pulsation state, has been widely observed in nonlinear systems [16–19].

Generally, period-doubling bifurcation takes place when a slight change in a system's parameters leads to the emergence of a new periodic orbit that doubles the period of the original orbit. Further, the cascade of period-doubling bifurcations manifests a well-known route to chaotic dynamics. Apart from their fundamental importance in nonlinear science, investigating period-doubling bifurcation is also attractive for potential applications, e.g., improving the spectroscopy accuracy as period doubling comes along with additional tones in a frequency comb [20, 21].

As a typical form of Hopf-bifurcation, period doubling in mode-locked fiber laser often arises in the region where pump power is higher than the threshold for stationary mode-locking. Note that oscillating dissipative solitons with long periods can also be observed in this pump power region, while as an obviously different periodic solution compared to period-doubling bifurcation. In this work, the oscillating soliton is defined as a solution with relatively weak spectral periodic variation, while its temporal intensity evolution is much more obvious. Simultaneously, the defined oscillating soliton normally exhibits longer periodicity from tens to hundreds of roundtrips. Thereby, although both the period doubling and oscillating dissipative solitons correspond to limit cycle attractors for nonlinear systems, the spectral evolution and oscillating period for period-doubling and defined oscillating solitons have clearly distinct features. The spectra of two successive roundtrips (RTs) in period doubling show obvious reversals of peak-to-dip, while those in oscillating states are absent. Another similar but yet different concept of dissipative soliton is the long-period extreme pulsation, namely, the breather [22, 23]. It is worth noting that this particular pulsation implies obvious spectral and temporal periodic variation, which mostly occurs with the pump power lower than the stationary mode-locking threshold [3].

Period doubling, multiple-period bifurcation, chaotic and other complicated pulsating solitons have been theoretically predicted by the complex cubic-quintic Ginzburg-Landau Eqs. [24–27]. However, early experimental observation of such fast pulsation soliton evolution was challenging due to the limited refresh rate of traditional measurement tools. Benefit from the rapid development of Time-stretch dispersive Fourier-transform (TS-DFT) technique [28–30], the single-shot spectral measurement allows real-time observation of transient and unrepeatable evolution of dissipative solitons. As a result, intriguing pulsation or oscillating solitons such as invisible solitons pulsation [31, 32], plentiful period-doubling bifurcation [33–35], and oscillating soliton molecular complexes [36, 37] have been revival and unveiled. However, to date, the explorations of period-doubling dissipative soliton were primarily restricted to the self-sustained steady regime. Although the spectral period doubling of dissipative soliton has been observed in diverse ultrafast laser configurations, there is still no consensus on its physical origin. Moreover, the spontaneous and controllable switching between period doubling and other intriguing dynamical states remain largely unexplored in experiments.

In this work, we explore the spectra periodic doubling of dissipative solitons via gain control, providing the first experimental demonstration of spontaneous, collisional and controllable spectral period-doubling dynamics in a polarization-maintaining (PM) mode-locked fiber laser. Several original features are highlighted. The spontaneous spectral period doubling can be observed with both single- and double-pulse at a critical pump region. Numerical simulation elucidates the dynamic switching of

periodic doubling and oscillating states. The corresponding period-doubling bifurcation is a quasi-stable state during switching rather than generally quickly converted to chaos through multi-period bifurcation. Moreover, the state transformation of individual solitons can be resolved during triple soliton collision involving stationary, oscillating and period-doubling states. Further, controllable deterministic switching between period doubling and other dynamical states is achieved under programmable pump modulation. The applicability of period-doubling-based digital encoding is further demonstrated in this platform. These findings open a new window for unveiling complex Hopf bifurcation in nonlinear systems and assist in improving laser performance.

Results

System configuration and principle

To investigate the spectral period doubling of dissipative solitons, an all polarization-maintaining Yb-doped mode-locked fiber laser is built as shown in the insert of Fig. 1a. The details of the experimental setup can be found in the method section. Apart from the stationary soliton singlet, a variety of stable states with oscillating or periodic-doubling operation can also be generated in the laser under sufficient gain supply, which is termed as oscillating single/double pulse (OSP/ODP), and double-pulse period doubling (DPD) (Fig. 1a). It is worth noting that another three particular transient states with dynamical period doubling characteristics can be observed at the critical pump region, which is termed transient period doubling (TPD-I, -II, -III) states. These diverse dissipative soliton behaviors are dominated by the energy variation of external pump strength, which is essential for gain-dominated soliton Hopf bifurcation. Among them, the oscillating pulse (OSP/ODP) with long periodicity corresponds to weak spectral and temporal periodic oscillation, while the periodic-doubling soliton (SPD, DPD) possesses conspicuous spectra variation over two consecutive roundtrips with spectral peak-to-dip flip.

Figure 1b suggests the versatile dissipative soliton states along the pump power increase. The evolution of soliton states related to pump strength is labeled by color bars, and the three transient states (green region in Fig. 1b) can only be observed at a particular pump region. During the single-pulse operation, a tiny increase in pump power leads the dissipative soliton transition from stationary single pulse (SSP) to oscillating state (OSP), while further increasing the pump power will trigger the soliton switching to a transient period doubling state (S-SPD). For double-pulse operation, a similar transient state (S-DPD) can also be observed involving oscillating and period-doubling. These two transient states both correspond to the spontaneous switching between oscillating and period doubling. Besides, a more complicated transient state is manifested in the edge of soliton doublets and triplets (C-PD), owing to the collision-induced state exchange involving period doubling, stationary and oscillating. It is worth noticing that the three transient states (green region in Fig. 1b) are first revealed in our work, to the best of our knowledge. The corresponding output power and pulse energy evolution along the pump increase are also shown in Fig. 1b. Pulse energy is calculated by dividing the measured output power by the pulse number observed via oscilloscope. Please note that this compact all PM fiber laser structure is immune to external polarization and environmental perturbations, thus intracavity gain supply plays the most crucial role in achieving

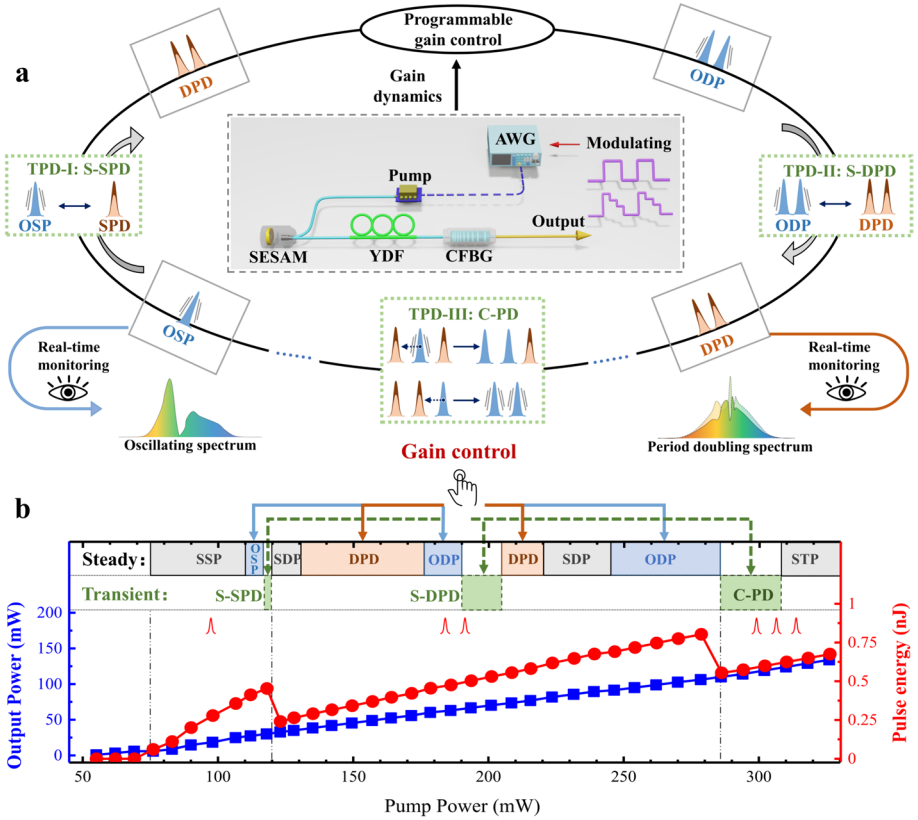

Fig. 1 Schematic configuration and dissipative soliton period doubling dynamics. **a** An ultrafast laser manipulation system including a mode-locked fiber laser, a programmable pump control and real-time detection module. The experimental setup for fiber laser is shown in the inset. The laser is mode-locked by SESAM and various mode-locking states can be achieved by adjusting the pump power. The gain supply is controlled by electronic modulation signals via an AWG. Real-time spectral and temporal detection of diverse soliton dynamics is implemented via dispersive fiber, photodetector, and fast oscilloscope. **b** Output power and pulse energy variations with the increased pump power and diverse soliton states are labeled by color bars along the pump power increase. AWG: arbitrary waveform generator; WDM: wavelength division multiplexer; SESAM: semiconductor saturable absorption mirror; YDF: ytterbium-doped fiber; CFBG: chirped fiber Bragg grating; OSP/ODP: oscillating single- and double-pulse; SPD/DPD: single and double pulse period doubling; C-PD: collisional period doubling; TPD: transient period-doubling; S-SPD/DPD: spontaneous single- and double-pulse period doubling; SSP, SDP, STP: stationary single, double, triple pulse.

specific soliton operation. Therefore, controllable fast switching between versatile states including period doubling and other dynamical states can be achieved by programming pump modulation.

Further, the RF spectrum can clearly manifest the plentiful soliton states along the pump power increase, as shown in Fig. 2a. For soliton singlet and doublet operation, stationary single- and double-pulse (SSP and SDP) can be generated at pump currents of 150 and 240 mA (as indicated by the arrow in Fig. 2a). With the increase of pump current to 224 and 360 mA, stable OSP and ODP states can be resolved, evidenced by the emergent RF sideband around the fundamental repetition rate of 66.2 MHz. It is worth noticing that two particular transient states (S-SPD and S-DPD) can be observed when the pump current increases to 235 and 381 mA, corresponding to the spontaneous switching between period-doubling and oscillating states. The appearance of

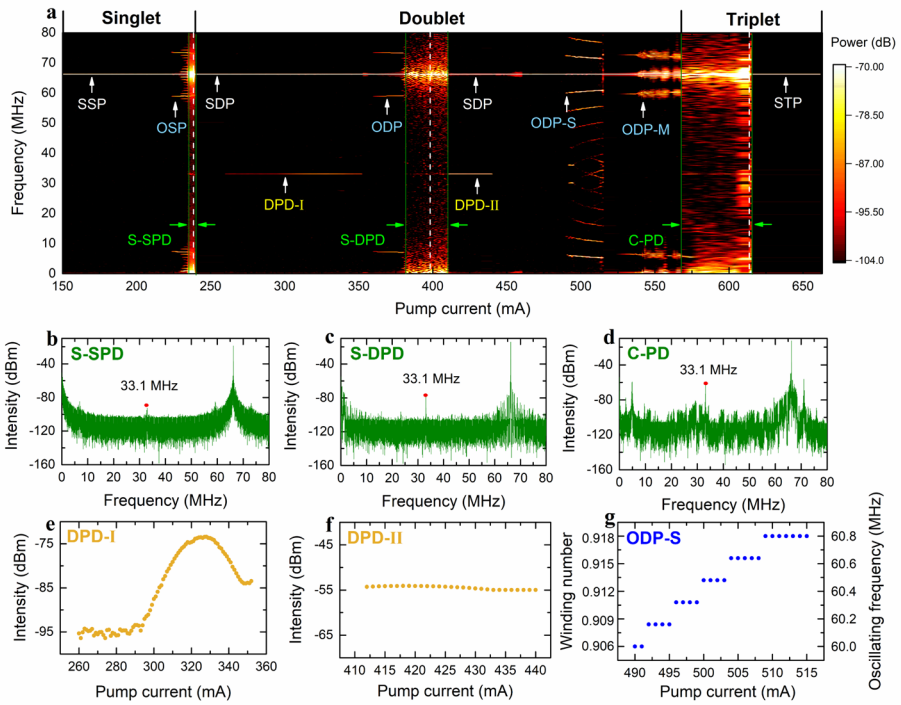

Fig. 2 Map of the laser spectral intensity in the space of RF and pump current, showing evolution of diverse soliton dynamics. **a** Measured RF spectrum as a function of pump current. SSP, SDP, STP: stationary single, double, triple pulse; OSP, ODP: oscillating single, double pulse; ODP-S, ODP-M: oscillating double pulse with shifting or multiple sidebands; DPD: double pulse period doubling; S-SPD, S-DPD: spontaneous single, double pulse period doubling; C-PD: collisional period doubling. **b-d** Single-shot RF spectra of S-SPD, S-DPD, and C-PD, showing transient behavior of period doubling and other states; **e-f** Intensity of RF sidebands along with pump current in DPD-I, DPD-II regime, showing changed and unchanged sideband intensity; **g** RF frequency and corresponding winding number of oscillating sideband in ODP-S, showing shifting sideband frequency along with pump current

subharmonic narrow peaks in the corresponding RF spectrum with a repetition rate of 33.1 MHz is the typical characteristic of period doubling (Fig. 2b and c). The coexistence of sidebands around the fundamental repetition rate and half of the repetition rate (33.1 MHz) verifies the spontaneous switching between two states. Please note that these particular transient behaviors only exist within the critical pump range. Further increase of pump current will break the delicate dynamical balance between oscillating and period-doubling states. As a result, the coexistence of the sidebands in RF spectrum will disappear, which implies dissipative soliton transitions to a steady state. Moreover, another intriguing transient state (C-PD) can be observed at the pump current of 569–615 mA, corresponding to the state exchange of individual solitons including period doubling, stationary, and oscillating states. The corresponding RF spectrum in Fig. 2d visibly shows the coexistence of subharmonic, oscillating and other unstable modulation sidebands. Besides the three kinds of transient states (S-SPD, S-DPD, and C-PD), the RF spectrum in Fig. 2a also suggests other intriguing diverse steady states such as double-pulse period doubling (DPD) with variable (Fig. 2e) or invariable (Fig. 2f) sideband intensity corresponding to a variation or quasi-stable pulsation ratio, and oscillating double pulses with shifting (ODP-S) or multiple (ODP-M) RF sidebands. Apart from intensity variation, frequency shifting of RF sidebands can also be observed. Figure 2g exhibits the oscillating

frequency evolution along with the pump increasing within ODP-S regime, the staircase-like increase of winding number corresponding to the Devil's staircase [4].

Spontaneous period doubling of single and double pulses

Besides the rich information provided by RF spectrum of transient and self-sustained steady soliton states, diverse dynamic regimes can also be experimentally resolved in real-time using TS-DFT technique, especially for transient period doubling states. As shown in Fig. 3a, the results measured by DFT indicate the spontaneous switching from oscillating single pulse to period-doubling and then reestablishes its original state (S-SPD in Fig. 2). The zoom-in plot of oscillating single soliton spectral evolution is shown in Fig. 3b with an oscillating period of 76 RTs. Meanwhile, the detailed spectra evolution of the period-doubling single soliton can be resolved in Fig. 3c (corresponding to the dashed rectangle in Fig. 3a). DFT spectra of two successive RTs (Fig. 3d) further verify the spectral period-doubling characteristics. The pulsation is manifested within a relatively broad soliton spectrum containing both center and tails, which is obviously different from the narrow band oscillation observed in the anomalous dispersion regime [31].

As verified in RF spectrum around pump currents of 400 mA (S-DPD in Fig. 2), the transient spontaneous period-doubling can also be observed within double-pulse

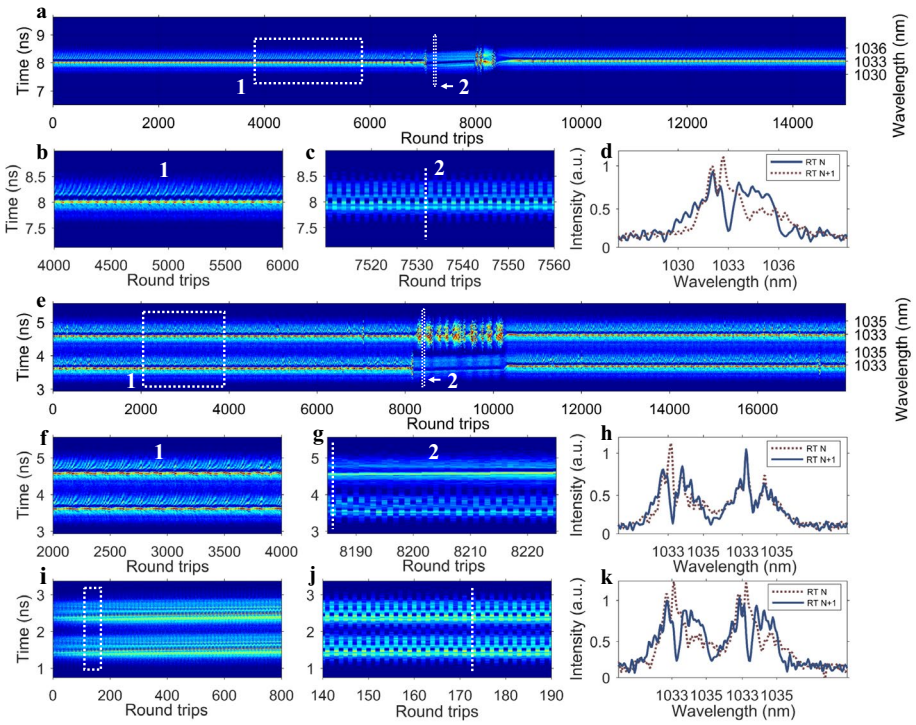

Fig. 3 Spontaneous period-doubling dynamics measured by DFT. **a** Spectra evolution for transient period doubling of single pulse. Zoom-in spectra of **b** oscillating single pulse and **c** single-pulse period doubling. **e** Spectra evolution for transient period doubling of double pulses. Zoom-in spectra of **f** oscillating double-pulse and **g** transient state with different behaviors of individual solitons. **i** Zoom-in spectra of double-pulse period doubling with synchronized pulsation characteristics for a different initial condition. **j** Zoom-in spectra of 50 RTs from **i**. **d**, **h**, **k** Single-shot spectra of two successive roundtrips from **c**, **g**, **j**

operation. The detailed spectral evolution of oscillating and period-doubling states for double-pulse at a pump power of 198 mW is shown in Fig. 3f and g, respectively. Before switching, the oscillating soliton pair exhibits periodic spectral evolution with an oscillating period of 168 RTs. Subsequently, the DFT spectra (Fig. 3g) indicate obviously different behaviors for the individual solitons in the transition state, which experience periodic doubling or chaotic evolution. Further, with a different initial condition, the spontaneous period doubling of two solitons can be observed in the experiment, as shown in Fig. 3i. Different from Fig. 3e, here, the detailed DFT spectral evolution (Fig. 3j) clearly indicates synchronous pulsation behavior for two solitons. The DFT spectra of two successive RTs in Fig. 3k further verify the synchronized period-doubling characteristics. Moreover, the spectral period-doubling of the dissipative soliton molecule can be found in Fig. S1 of the supplementary material.

To corroborate the experimental observations and unveil the physical origin, the soliton switching between long-period oscillating (LPO) and period-doubling (Fig. 3a), we execute numerical simulations based on a lumped scalar model for the laser configuration and parameters. More details of the modeling are presented in the method section. For the parameters set defined with $E_s = 6.1$ pJ, the soliton switching dynamics between long-period oscillating and period-doubling can be resolved in Fig. 4a. The LPO soliton first generated in simulation at this critical pump strength and the corresponding spectra evolution over cavity roundtrips is shown in Fig. 4a from RT 1 to 1860. Figure 4b exhibits the simulated single-shot optical spectrum of the LPO soliton, reproducing the experimental results convincingly (Fig. 4c corresponding to the single-shot spectrum in Fig. 3b). Subsequently, the LPO soliton switches to period-doubling (RT 2000 to 2060) and then recovers to the original oscillating state (RT 3000 to 5000). The detailed spectra and energy evolution (white curve) of period-doubled soliton are shown in Fig. 4d. The obvious pulsations can be resolved in this net-normal dispersion regime, which is different from the reported "invisible" pulsation in the anomalous dispersion regime [31]. Two consecutive output optical spectra and temporal intensity profiles are shown in Fig. 4e and f, respectively. The conspicuous differences in their spectral shape further

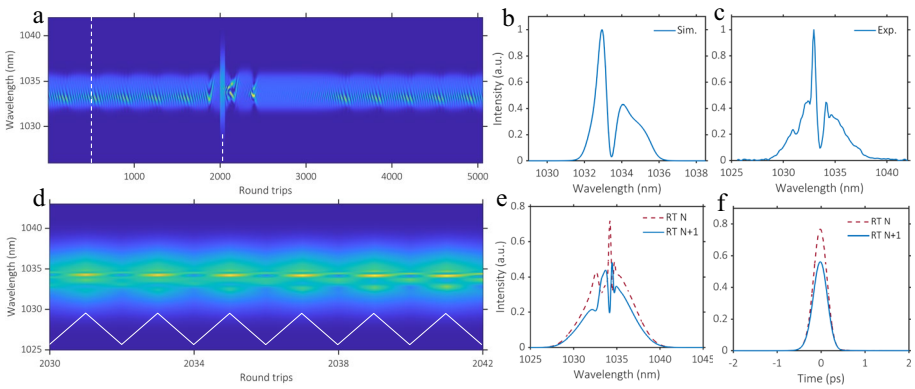

Fig. 4 Simulation results of spontaneous soliton switching between long-period oscillating and period doubling. **a** Simulated spectra evolution of soliton switching between LPO and period doubling. Single-shot optical spectra of long-period oscillating soliton in **b** simulation and **c** experiment. **d** Zoom-in plot of the spectra evolution in **a** corresponding to soliton period doubling operation. **e** Two consecutive optical spectra and **f** temporal intensity profile of output pulse

demonstrate the period-doubling characteristics. The corresponding simulation result of intracavity light field evolution and chirp characteristic in period doubling operation can be found in Figs. S2 and S3 of the supplementary material.

Period doubling dynamics during triple-pulse collision

Remarkably, another type of transient soliton state switching involving period doubling during multiple soliton collision can be observed at the pump power of 290 mW (C-PD in Fig. 2), as depicted in Fig. 5. For the triple-soliton collision shown in Fig. 5b, leading and trailing solitons correspond to period-doubling state (Fig. 5a), and the middle soliton exhibits an oscillating state while with different group velocity compared to the other two solitons. This group velocity difference is induced by the intracavity gain-dependent filtering effect, thereby resulting in a collision between leading and middle solitons. During the collision, the oscillating soliton collided with the nearby period-doubling soliton and then merged to be a single stationary soliton, demonstrating the inelastic collision characteristics. Simultaneously, as a global intracavity perturbation induced by the collision, the trailing period-doubling soliton was split into a stationary soliton and a new period-doubling soliton. The detailed spectral evolutions before and after collision are shown in Fig. 5a and c, further demonstrate multiple solitons state switching involving stationary, period-doubling and oscillating states. Moreover, with a different initial condition, the collision between different pulses can result in state transformation for individual pulses and a decrease in pulse number, as shown in Fig. 5e. Before the triple-soliton collision, two solitons possess the period-doubling evolution while the trailing soliton exhibits the stationary state (Fig. 5d). Similarly, due to the group velocity difference between the period-doubling soliton pair and the stationary soliton, the trailing

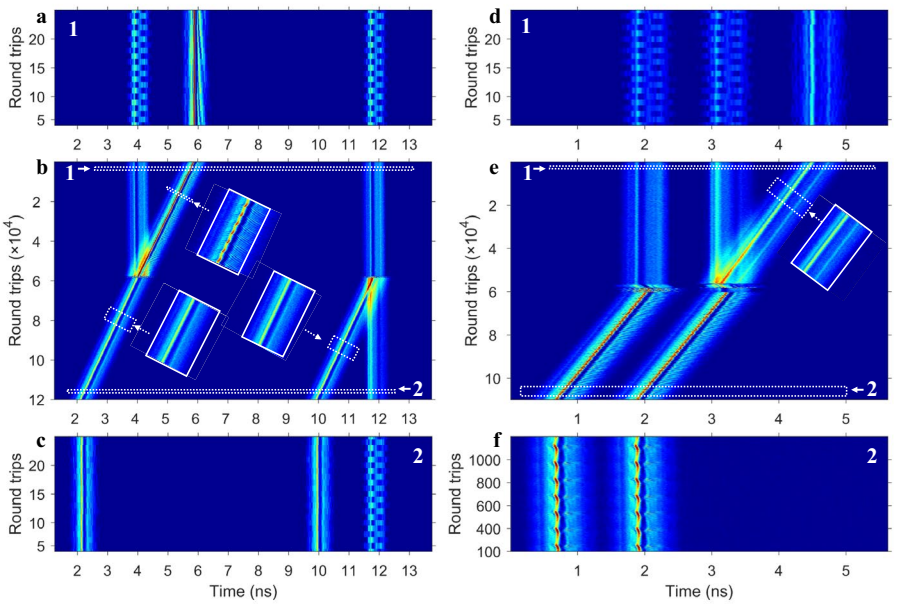

Fig. 5 Collisional period-doubling dynamics of triple-pulse. **a** Initial 20 roundtrips evolution in **b**. **b** Real-time spectra evolution without soliton number change measured via DFT. **c** Final 20 roundtrips evolution in **b**. **d** Initial 20 roundtrips evolution in **e**. **e** Real-time spectra evolution with soliton number change measured via DFT. **f** Final 20 roundtrips evolution in e

stationary soliton collided with the nearby period-doubling soliton and merged to be a single oscillating soliton. Meanwhile, the leading period-doubling soliton switches to an oscillating state due to global energy perturbation. The finally generated two oscillating solitons after collision have the same oscillating period of 150 RTs, as shown in Fig. 5f. More cases of the synchronous and asynchronous period-doubling soliton pair before the triple-soliton collision can be found in Fig. S4 of supplementary material. Under a higher pump power, the self-sustained stable period-doubling three and four solitons can also be observed, as shown in Figs. S5 and S6 of supplementary material, respectively.

Controllable period doubling under pump modulation

As observed in the above section, linear increase or decrease in pump power results in the switching between period-doubling and other dynamics states (Fig. 1b). Thereby, programmable electronic modulations of the pump gain are applicable to achieve controllable switching of dissipative solitons involving period-doubling state. Here, we design a periodic electronic signal to modulate the pump power and achieve deterministic continuous switching between different states of dissipative solitons. Firstly, under the pump power of 132 mW and modulation frequency of 10 kHz, periodic switching of the dissipative soliton is realized. The temporal intensity and DFT spectra evolutions are shown in Fig. 6a and b, respectively. During each period, the oscillating single soliton switches to a period-doubling soliton pair when the pump strength is modulated to a higher value. Meanwhile, pulse temporal separation of period-doubling soliton pair is gradually increased due to the intense repulsive effect. The detailed spectral evolutions of soliton oscillating and period-doubling are shown in Fig. 6c (corresponding to the dashed rectangle in Fig. 6b), further demonstrating the obviously different spectral characteristics of two operation states. Similarly, at the pump power of 170 mW and modulation frequency of 10 kHz, the periodic switching between oscillating and period-doubling soliton pairs with constant temporal interval can be resolved in Fig. 6d and e. The detailed spectral evolutions of two different states are shown in Fig. 6f. The periodic temporal and spectral evolutions (Fig. 6a, b, d and e) demonstrate the controllable and reversible switching between period doubling and other dynamic states. The two successive single-shot spectra shown in Fig. 6m and n further demonstrate the spectral period-doubling characteristics.

Besides the continuous switching between two states, the multi-state switching of dissipative solitons can also be realized by programming the electric modulating signal. At the pump power of 188 mW and three-level modulation frequency of 5 kHz, continuous switching of soliton between three different states can be resolved, the corresponding temporal intensity and spectral evolutions are shown in Fig. 6g and h. As the lowest pump power corresponds to the lowest modulation voltage, laser output manifests as an oscillating single soliton. An abrupt increase in pump power induces the generation of double pulses period-doubling with intense repulsive interaction in the temporal domain. Subsequently, a slight decrease in the pump strength leads to the state of oscillating double-pulse with constant temporal interval. The corresponding spectral evolutions of the three states are shown in Fig. 6i. Similarly, at the pump power of 300 mW and four-level modulation frequency of 5 kHz, the consecutive switching between four

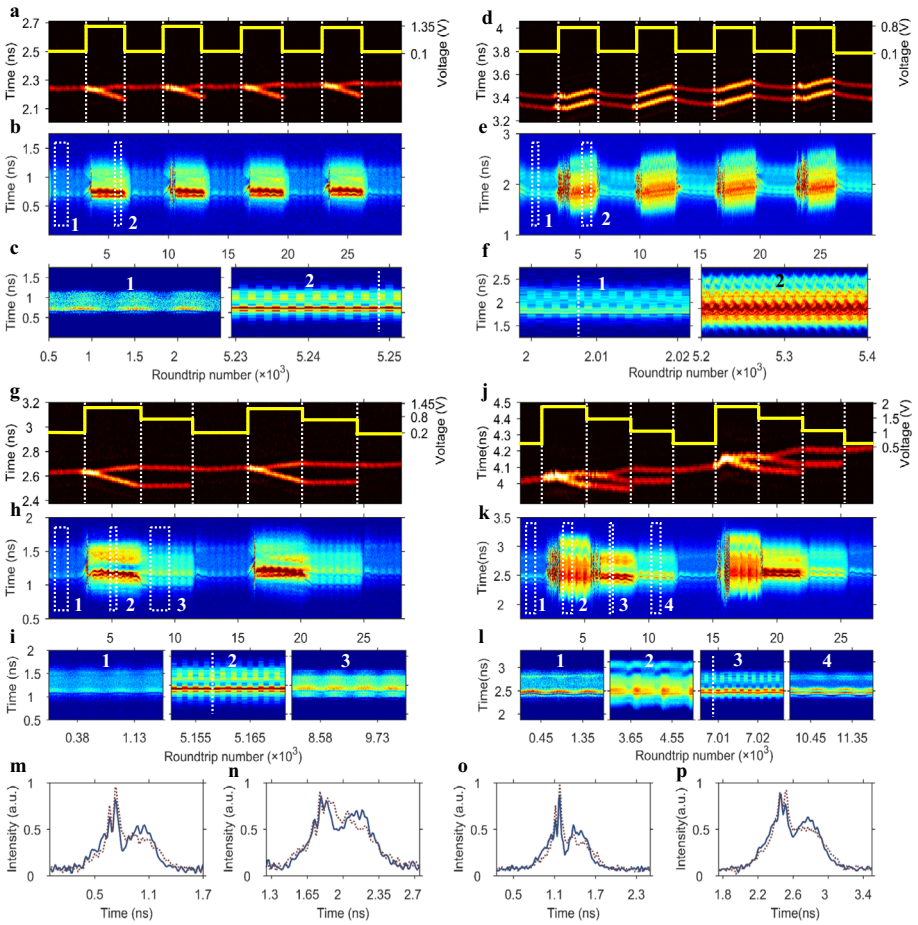

Fig. 6 Consecutive switching of period doubling and other states under periodic pump modulation. **a-c** Consecutive switching between OSP and DPD by a modulation frequency of 10 kHz. **d-f** Consecutive switching between ODP and DPD by a modulation frequency of 10 kHz. **g-i** Consecutive switching of three different states by a modulation frequency of 5 kHz. **j-l** Consecutive switching of four different states by a modulation frequency of 5 kHz. **a**, **d**, **g**, **j** Temporal intensity evolution and embedded modulated electronic signal. **b**, **e**, **h**, **k** Real-time spectral evolution measured via DFT. **m**, **n**, **o**, **p** DFT spectra of two successive roundtrips

different states can be achieved, as shown in Fig. 6j and k. Four soliton evolution states can be clearly identified with the pump power variation in one period, including oscillating single pulse, two oscillating double-pulse states with different temporal and spectral characteristics, and triple-pulse period doubling. The corresponding detailed spectral evolution of each state is shown in Fig. 6l.

The controllable fast switching of dissipative solitons with versatile spectral characteristics is beneficial for potential applications in optical computing, information encoding, and soliton communication [38, 39]. As a proof of concept, we conducted the digital coding using two steady soliton states: the oscillating single pulse ('0') and double-pulse period doubling ('1') (the same state in Fig. 6a). The conversion of OSP and DPD can be achieved by changing the pump current of the fiber laser. As a result, the optical binary codes of HKU (010010000100101101010101, an abbreviation from the University of Hong Kong) and ABIC (010000010100001001001001010000011, an abbreviation from

Advanced Biomedical Instrumentation Centre) can be obtained by programming the pump current, as shown in Fig. 7a. Each letter can be encoded by 8 bits with a total temporal duration of 800 μs, corresponding to the encoding frequency of several kHz, which is significantly improvement compare to the manually adjust the polarization controller (~ several Hz) [39]. It should be noted that the transition period for soliton states switching is ~ 1300 RT, corresponding to a hysteresis time of 20 μs, which implies the higher switching frequency for our laser is also achievable (~ 50 kHz). For visualization, the corresponding multi-letter streams are shown in Fig. 7(b). This multi-letter test further verifies the availability of periodic-doubling-based digital encoding in this platform and the potential for a higher capacity in all-optical storage.

Conclusions

Period-doubling as an exotic state, generally indicates the existence of chaotic dynamics in the vicinity of the system parameters. In this work, we further extend the physical origin of the period doubling in an all-PM mode-locked fiber with a linear structure. Unlike the narrow-band pulsation observed in the anomalous dispersion fiber laser [31], the period doubling in our laser with net-normal dispersion is manifested with a relatively wide band pulsation on the soliton spectrum containing both center and tails. Numerical simulations reproduce the experimental results convincingly, demonstrating that the Kerr nonlinearity plays a vital role in these period-doubling operations. The composite effects of SA response and nonlinearity induced in gain fiber shape the pulse with obviously different output spectral characteristics over two consecutive roundtrips.

Moreover, for the reported conventional period doubling [32], the orderly soliton, which corresponds to a stationary period-1 mode-locking regime, gradually transitions to period-doubling bifurcation, period-N bifurcation, destabilization, and chaos as continuously increasing the pump power. Whereas soliton experiences a regular transition in our experiment including stationary, oscillating, and period-doubling states, overdrive of the pump power only induces pulse splitting without the occurrence of chaos. Benefiting from these regular transitions in this all-PM fiber laser, the interesting spontaneous switching between oscillating and period-doubling can be observed in the single or double-pulse at the critical pump region. In addition, the state exchange of individual solitons can be resolved during the inelastic collision of triple solitons involving stationary, oscillating, and period-doubling states. The group velocity difference of triple solitons at this particular pump regime is attributed to the gain-dependent filtering effect. Thereby, the continuous collision can either enable the operation state change of individual soliton or cause the decrease of soliton number after mutual interaction.

Further, the controllable switching of period-doubling and other dynamical states can be achieved by precisely programming pump modulation. In contrast to the state switching in fiber laser mode-locked by nonlinear polarization rotation, the all-PM fiber laser can easily exclude polarization and environmental perturbations. Thus, the consecutive deterministic switching of dissipative solitons between different limit-cycle attractors was demonstrated involving oscillating and period-doubling states under tailored pump modulation. The exhibited exemplary string ('HKU' and 'ABIC') experimentally validates the availability of this periodic-doubling-based digital encoding. Moreover, the controllable fast switching of diverse soliton states (period-doubling or long period oscillating)

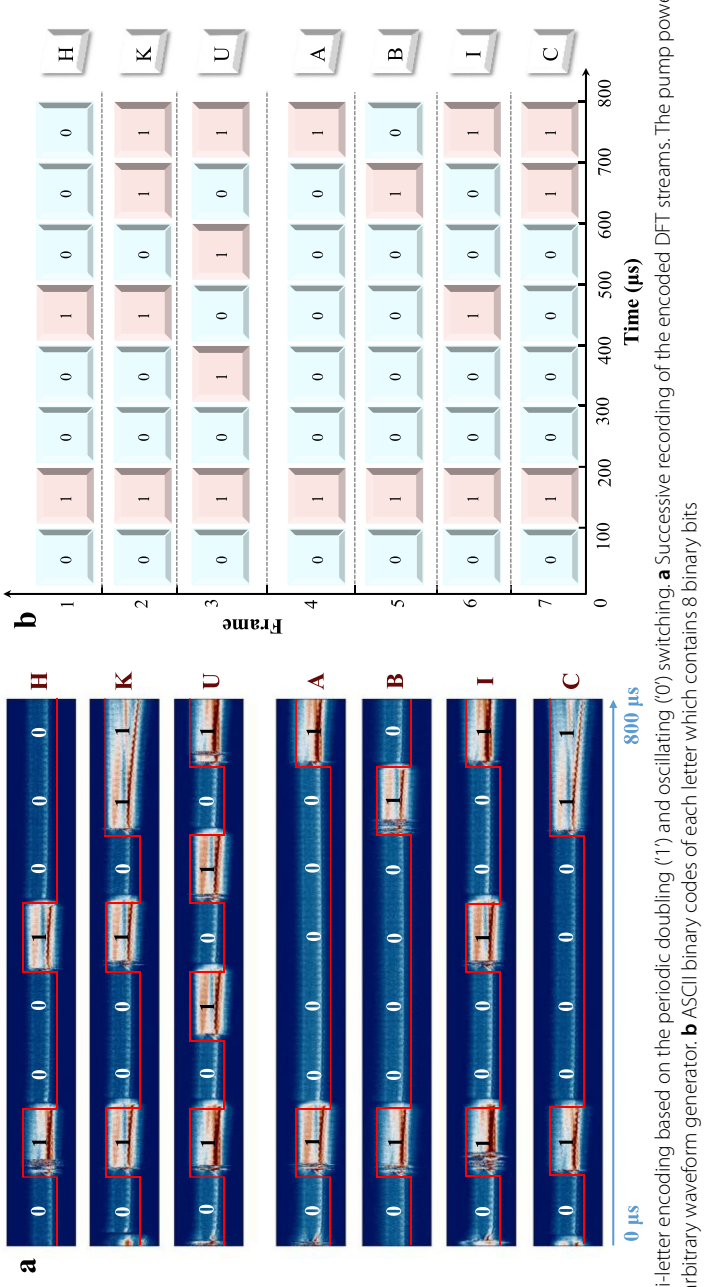

Fig. 7 Exemplary multi-letter encoding based on the periodic doubling ('1') and oscillating ('0') switching. **a** Successive recording of the encoded DFT streams. The pump power is set at 130 mW and modulated by an arbitrary waveform generator. **b** ASCII binary codes of each letter which contains 8 binary bits

gives rise to a flexible selection of laser spectrum with sparse or dense RF comb teeth, which can be regarded as frequency-modulated pulsed laser, thus holds great potential for applications in coherent laser ranging [40].

Potentially, our work may stimulate the study of the period-doubling bifurcation in other physical systems. The investigation of dissipative soliton switching between different attractors (period-doubling or oscillating) through programming pump modulation can also be extended to other laser cavities with different mode-locking schemes and configurations. Our results generalize previous observations made in the case of steady period doubling in ultrafast lasers. We believe that our findings will stimulate further research on the complex Holf-bifurcation enabled in dissipative systems and assist in improving laser performance.

Methods

Experimental setup

The Yb-doped fiber laser (Fig. 1a) used in this experiment containing an integrated multi-functional element, a piece of Yb-doped fiber (PM-YSF-HI-HP) and a chirped fiber Bragg grating (CFBG). The multi-functional element includes a fiber pigtailed semiconductor saturable absorber mirror (SESAM, SAM-1030-55-500 fs) and a 976/1030-nm wavelength-division multiplexer (WDM). The gain fiber is pumped by a 976-nm laser diode with maximum average power of 400 mW. The length of gain fiber is 0.85 m while the length of residual single-mode fiber (PM980) in the cavity is 0.66 m. The CFBG (DMR-1030-20-25-P1) can provide an anomalous dispersion of 0.0338 ps^2, thus the net cavity dispersion of our laser is ~0.0304 ps^2. The reflection bandwidth of CFBG is 20 nm centered at 1030 nm, which also acts as an output coupler with an output ratio of 70%. All the elements in the laser cavity are polarization-maintaining devices. Therefore, stable mode-locking state can be obtained by simply increasing the pump power. Passive mode-locking operation is realized by the fast saturable absorber with the relaxation time constant of ~500 fs. A fiber optical coupler (OC) is spliced after CFBG to divide the output pulse, which measures the pulse spectral information through an optical spectrum analyzer (Agilent, 86142B) and undispersed temporal information through a high-speed oscilloscope (Keysight, DSOV204A) with a photo-detector (12.5 GHz bandwidth). To investigate the real-time soliton evolution dynamics, a 1-km single-mode fiber (HI1060) is equipped before another photo-detector (12.5 GHz bandwidth) to achieve the wavelength-to-time conversation for measurements via the TS-DFT technique. The temporal and spectral resolution of this experiment is 80 ps and 0.43 nm, respectively [41]. Although higher spectral resolution can be achieved by using longer dispersion fiber, it will cause information loss due to the overlap of stretched multi-pulse. Current spectral resolution in our TS-DFT is sufficient for resolving soliton behavior in the multi-pulse state without obvious cross-talk.

Numerical simulation

The propagation of solitons within the fiber section is modeled with a generalized nonlinear Schrödinger equation in the scalar approach, which takes the following form.

$$\frac{\partial u(z,t)}{\partial z} = -i\frac{\beta_2}{2}\frac{\partial^2 u(z,t)}{\partial t^2} + \frac{g}{2\Omega_g^2}\frac{\partial^2 u(z,t)}{\partial t^2} + i\gamma|u(z,t)|^2\,u(z,t) + \frac{g}{2}u(z,t) \tag{1}$$

Here u is the slowly varying envelope moving at the group velocity along the propagation coordinate z; β_2 and γ are the second-order dispersion coefficients and Kerr nonlinearity, respectively; Ω_g is the gain bandwidth. In the passive single-mode fiber, we set gain $g=0$. In the case of Yb-doped fiber, the gain is described using the formula:

$$g = g_0 \exp\left(-\frac{E_p}{E_s}\right) \tag{2}$$

Where g_0 is the small signal gain, E_p is the pulse energy, and E_s is the gain saturation energy determined by pump power. The commercialized SESAM and CFBG is modeled by the following form:

$$u_{SESAM} = F^{-1}\left\{F[u(L_c,t)]e^{iL_{SAM}(\omega)}\sqrt{R_{SAM}(\omega)/(1-q_a-q_0)}\right\}\sqrt{(1-q_a-q)\eta_{SAM}} \tag{3}$$

$$\frac{\partial q}{\partial t} = \frac{q-q_0}{\tau_a} - q\frac{|u(L_c,t)|^2}{E_a} \tag{4}$$

$$u(0,t) = F^{-1}\left\{F[u(2L_c,t)]e^{iL_{FBG}(\omega)}\sqrt{1-q_{FBG}}\right\} \tag{5}$$

Where u_{SESAM} represents the light field $u(L_c,t)$ after being modulated by the SESAM, L_c represents the cavity length, the operator $L_{SAM}(\omega)$ and $L_{FBG}(\omega)$ accounts for the dispersion of the SESAM and CFBG, respectively. $R_{\mathrm{SAM}}(\omega)$ is the wavelength-dependent low-intensity spectral reflectance of the SESAM. q_{a}, q_0, E_{a}, τ_{a}, η_{SAM} are the unsaturable loss, modulation depth, saturation energy, relaxation time, and coupling efficiency of SESAM, respectively. The CFBG, as an output coupler, dispersion compensation device, and filter simultaneously, has a high reflectance and transmits only a fraction of the signal characterized by q_{FBG} (output ratio). Simultaneously, the spectral filtering effect induced by the CFBG was modeled by a 20 nm Gaussian filter. The initial seed condition was a white noise field. During simulation, the parameter E_{s} was just varied, determined by pump power to achieve the different lasing states. The parameters used in the simulation follow typical values: $g_0=3.5\ \mathrm{m}^{-1}$, $\Omega_{\mathrm{g}}=50$ nm, $E_{\mathrm{a}}=22$ pJ, $R_{\mathrm{SAM}}=0.7$, $q_0=0.30$, $\tau_{\mathrm{a}}=0.7$ ps, $q_{\mathrm{FBG}}=0.7$.

Abbreviations

RT	roundtrip
TS-DFT	time-stretch dispersive Fourier-transform
PM	polarization-maintaining
OSP/ODP	oscillating single- and double-pulse
SPD/DPD	single and double pulse period doubling
C-PD	collisional period doubling
TPD	transient period-doubling
S-SPD/DPD	spontaneous single- and double-pulse period doubling
SSP, SDP, STP	stationary single, double, triple pulse
AWG	arbitrary waveform generator
WDM	wavelength division multiplexer
SESAM	semiconductor saturable absorption mirror
YDF	ytterbium-doped fiber

CFBG	chirped fiber Bragg grating
RF	radio frequency
ODP-S, ODP-M	oscillating double pulse with shifting or multiple sidebands
LPO	long-period oscillating
HKU	the University of Hong Kong
ABIC	advanced biomedical instrumentation centre
SA	saturable absorber

Supplementary Information

The online version contains supplementary material available at https://doi.org/10.1186/s43074-024-00141-8.

Supplementary Material 1.

Acknowledgements
We thank Prof. Philippe Grelu for fruitful discussions.

Authors' contributions
K.Y., Y.Z. conceived and performed the most experiments and simulations. K.K.T., H.Z., and K.K.Y.W. supervised and guided the project. K.Y., Y.Z., Y.L., K.K.T., H.Z., and K.K.Y.W. discussed the results and contributed to the writing of the paper.

Funding
This work was supported by National Natural Science Foundation of China (12374402), Research Grants Council of the Hong Kong Special Administrative Region of China (HKU 17210522, HKU C7074-21G, HKU 17205321, HKU 17200219, MHP/073/20, MHP/057/21) and Health@InnoHK program of the Innovation and Technology Commission of the Hong Kong SAR Government.

Availability of data and materials
The data supporting the plots within the paper and other findings of this study are available from the corresponding author upon reasonable request.

Declarations

Ethics approval and consent to participate
There is no ethics issue for this paper.

Consent for publication
All authors agreed to publish this paper.

Competing interests
The authors declare no competing interests.

Received: 15 May 2024 Revised: 13 August 2024 Accepted: 28 August 2024
Published online: 26 September 2024

References

1. Grelu P, Akhmediev N. Dissipative solitons for mode-locked lasers. Nat Photonics. 2012;6:84–92.
2. Akhmediev N, Ankiewicz A. Dissipative solitons: from optics to biology and medicine. Berlin Heidelberg: Springer; 2008.
3. Peng J, Boscolo S, Zhao Z, Zeng H. Breathing dissipative solitons in mode-locked fiber lasers. Sci Adv. 2019;5: eaax1110.
4. Wu X, et al. Farey tree and devil's staircase of frequency-locked breathers in ultrafast lasers. Nat Commun. 2022;13:5784.
5. Zhou Y, Ren YX, Shi J, Wong KKY, et al. Breathing dissipative soliton molecule switching in a bidirectional mode-locked fiber laser. Adv Photonics Res. 2022;3:2100318.
6. Herink G, Kurtz F, Jalali B, Solli DR, Ropers C. Real-time spectral interferometry probes the internal dynamics of femtosecond soliton molecules. Science. 2017;356:50–4.
7. Krupa K, Nithyanandan K, Andral U, Tchofo-Dinda P, Grelu P. Real-time observation of internal motion within ultrafast dissipative optical soliton molecules. Phys Rev Lett. 2017;118: 243901.
8. Liu X, Yao X, Cui Y. Real-time observation of the buildup of soliton molecules. Phys Rev Lett. 2018;121: 023905.
9. Zhou Y, Ren YX, Shi J, Mao H, Wong KKY. Buildup and dissociation dynamics of dissipative optical soliton molecules. Optica. 2020;7:965–72.
10. Runge AFJ, Broderick NGR, Erkintalo M. Observation of soliton explosions in a passively mode-locked fiber laser. Optica. 2015;2:36–9.
11. Zhou Y, Ren YX, Shi J, Wong KKY. Breathing dissipative soliton explosions in a bidirectional ultrafast fiber laser. Photonics Res. 2020;8:1566–72.
12. Liu M, Li TJ, Luo A, Xu WC, Luo ZC. Periodic soliton explosions in a dual-wavelength mode-locked Yb-doped fiber laser. Photonics Res. 2020;8:246–51.

13. Zhou Y, et al. Unveiling laser radiation of multiple optical solitons by nonlinear fourier transform. Laser Photonics Rev. 2023;17: 2200731.
14. Solli DR, Ropers C, Koonath P, Jalali B. Optical rogue waves. Nature. 2007;450:1054–7.
15. Lecaplain C, Grelu P, Soto-Crespo JM, Akhmediev N. Dissipative rogue waves generated by chaotic pulse bunching in a mode-locked laser. Phys Rev Lett. 2012;108: 233901.
16. Strogatz SH. Nonlinear dynamics and chaos: with applications to physics, biology, chemistry, and engineering. 2nd ed. Florida: CRC; 2015.
17. Erneux T, Kovanis V, Gavrielides A, Alsing PM. Mechanism for period-doubling bifurcation in a semiconductor laser subject to optical injection. Phys Rev A. 1996;53:4372–80.
18. Sucha G, Bolton SR, Weiss S, Chemla DS. Period doubling and quasi-periodicity in additive-pulse mode-locked lasers. Opt Lett. 1995;20:1794–6.
19. Zhao B, Tang DY, Zhao LM, Shum P, Tam HY. Pulse-train nonuniformity in a fiber soliton ring laser mode-locked by using the nonlinear polarization rotation technique. Phys Rev A. 2004;69: 043808.
20. Liao P, et al. Chip-scale dual-comb source using a breathing soliton with an increased resolution. In: Conference on lasers and electro-optics. San Jose: Optica Publishing Group; 2018.
21. Wu H, et al. Optical frequency combs based on a period-doubling mode-locked Er-doped fiber laser. Opt Express. 2018;26:577–85.
22. Cole DC, Papp SB. Subharmonic entrainment of Kerr breather solitons. Phys Rev Lett. 2019;123: 173904.
23. Peng J, et al. Breather molecular complexes in a passively mod-locked fiber laser. Laser Photonics Rev. 2021;15:2000132.
24. Chang W, Soto-Crespo JM, Vouzas P, Akhmediev N. Extreme soliton pulsations in dissipative systems. Phys Rev E. 2015;92: 022926.
25. Akhmediev N, Soto-Crespo JM, Town G. Pulsating solitons, chaotic solitons, period doubling, and pulse coexistence in mode-locked lasers: complex Ginzburg-Landau equation approach. Phys Rev E. 2001;63: 056602.
26. Soto-Crespo JM, Akhmediev N, Ankiewicz A. Pulsating, creeping, and erupting solitons in dissipative systems. Phys Rev Lett. 2000;85:2937–40.
27. Hennig D. Periodic, quasiperiodic, and chaotic localized solutions of a driven, damped nonlinear lattice. Phys Rev E. 1999;59:1637–45.
28. Goda K, Jalali B. Dispersive fourier transformation for fast continuous single-shot measurements. Nat Photonics. 2013;7:102–12.
29. Desbois J, Gires F, Turnois P. A new approach to picosecond laser pulse analysis shaping and coding. IEE J Quantum Electron. 1973;9:213–8.
30. Wu X, Peng J, Boscolo S, Finot C, Zeng H. Synchronisation, desynchronisation, and intermediate regime of breathing solitons and soliton molecules in a laser cavity. Phys Rev Lett. 2023;131:263802.
31. Liu M, et al. Visualizing the 'invisible' soliton pulsation in an ultrafast laser. Laser Photonics Rev. 2020;14:1900317.
32. Wang Z, Coillet A, Hamdi S, Zhang Z, Grelu P. Spectral pulsations of dissipative solitons in ultrafast fiber lasers: period doubling and beyond. Laser Photonics Rev. 2023;17: 2200298.
33. Cui Y, et al. XPM-induced vector asymmetrical soliton with spectral period doubling in mode-locked fiber laser. Laser Photonics Rev. 2021;15:2000216.
34. Xiao X, Ding Y, Fan S, Zhang X, Yang C. Spatiotemporal period-doubling bifurcation in mode-locked multimode fiber lasers. ACS Photonics. 2022;9:3974–80.
35. Zhao LM, Tang DY, Lin F, Zhao B. Observation of period doubling bifurcations in a femtosecond fiber soliton laser with dispersion management cavity. Opt Express. 2004;12:4573–8.
36. Wang ZQ, Nithyanandan K, Coillet A, Tchofo-Dinda P, Grelu P. Optical soliton molecular complexes in a passively mode-locked fibre laser. Nat Commun. 2019;10:830.
37. Zhou Y, Shi J, Ren YX, Wong KKY. Reconfigurable dynamics of optical soliton molecular complexes in an ultrafast thulium fiber laser. Commun Phys. 2022;5:302.
38. Liu Y, et al. Phase-tailored assembly and encoding of dissipative soliton molecules. Light Sci Appl. 2023;12:123.
39. Yang Z, et al. Ultrafast laser state active controlling based on anisotropic quasi-1D material. Light Sci Appl. 2024;13:81.
40. Riemensberger J, et al. Massively parallel coherent laser ranging using a soliton microcomb. Nature. 2020;581:164–70.
41. Tsia KK, Goda K, Capewell D, Jalali B. Performance of serial time-encoded amplified microscope. Opt Express. 2010;18:10016–28.

Publisher's note